Available online at www.sciencedirect.com
ScienceDirect
Thin Solid Films 515 (2006) 425 – 429
thin solid films
www.elsevier.com/locate/tsf

The effect of argon pressure on the structural and photocatalytic characteristics of TiO_2 thin films deposited by d.c. magnetron sputtering

K. Eufinger [a,*], E.N. Janssen [a], H. Poelman [a], D. Poelman [a], R. De Gryse [a], G.B. Marin [b]

[a] *Surface Physics and Thin Film Division, Department of Solid State Sciences, Ghent University, Krijgslaan 281-S1, 9000 Gent, Belgium*
[b] *Laboratorium voor Petrochemische Techniek, Department of Chemical Engineering, Ghent University, Gent, Belgium*

Available online 19 January 2006

Abstract

TiO_2 thin films of 200–300 nm thickness were deposited by d.c. magnetron sputtering onto glass substrates from a semiconducting TiO_{2-x} target in pure Ar using pressures between 0.1 and 1.0 Pa. The obtained TiO_2 coatings are transparent and have refractive indices between 2.5 and 1.9. Post deposition heat treatment at different temperatures was performed to achieve crystallization of anatase TiO_2. The as-deposited and heat treated films were examined with UV–VIS (transmission), SEM and XRD to investigate the influence of the argon pressure during deposition on the structural development during heat treatment. Additionally, the photocatalytic activity of the films was tested by measuring the decomposition rate of ethanol in a controlled gas atmosphere simulating air, and was related to their respective microstructures.

PACS: 81.15.Cd; 81.40.Ef; 82.65.+r
Keywords: TiO_2; d.c. magnetron sputtering; Microstructure; Photocatalysis

1. Introduction

TiO_2 is a large band gap semiconductor which has gained a lot of importance as catalyst for breakdown of organic substances under UV illumination. It is a chemically and biologically inert material with good photostability [1,2].

Of the three main crystal phases of TiO_2, rutile is the thermodynamically stable phase, but anatase and brookite have a high kinetic stability. In thin film processing usually the anatase phase is formed at temperatures below ca. 873 K [1]. It was shown that anatase (bandgap = 3.2 eV) is the more active phase in photocatalysis compared to rutile (bandgap = 3.0 eV) [1]. On the other hand, it has been argued that a mixture of anatase and rutile may show the highest photocatalytic activity; an example is the P25 powder from Degussa [3,4]. About the brookite phase very little is known. Therefore, most studies discuss pure anatase thin films.

In the photocatalytic process the TiO_2 is activated by illumination with UV light having an energy higher than the band gap. The photocatalytic break down reaction proceeds via intermediate steps ending in the mineralization of the organic to water, CO_2 and mineral acids. It is clear that there will be different factors influencing the various steps of the reaction. The initial step is the electron-hole pair formation, followed by their separation. The electrons can be used for reduction, the holes for oxidation processes [1]. The lifetimes of the electron and of the hole have an influence on how well they can be utilized for the subsequent redox-reaction. Structural imperfections in the TiO_2 lattice generate trap sites and recombination centers, leading to a decrease of the electron and hole concentration [1,4]. This means that amorphous and very small grained (<10 nm) TiO_2 are expected to show a lower photoactivity.

The most important factor for the chemical activity of a catalyst is the number of active sites. Among other things, this depends on the total available surface area [1], which can be controlled through the microstructure of the thin film: a dense and smooth film will have only the geometrical surface area, while loosely packed small grains result in a large surface area. The grains should be not too small, though, to keep the number of defects low. Therefore, it is aimed to achieve a high degree of crystallinity in the films while keeping the grain size well below 100 nm. The grains should also not be packed too loosely to ensure a wear resistant coating.

* Corresponding author. Tel.: +32 9 264 4343; fax: +32 9 264 4996.
E-mail address: karin.eufinger@ugent.be (K. Eufinger).

0040-6090/$ - see front matter © 2005 Elsevier B.V. All rights reserved.
doi:10.1016/j.tsf.2005.12.247

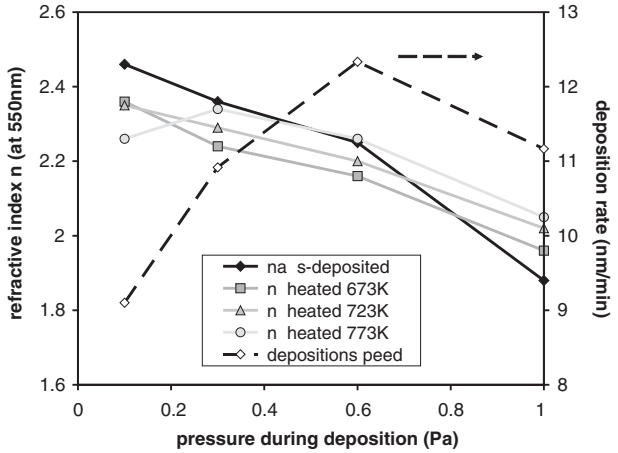

Fig. 1. Dependence of refractive index n at 550 nm (left axis) and deposition rate on the deposition pressure.

In this study TiO_2 thin films have been deposited by d.c. magnetron sputtering. This technique allows for deposition of well adherent, transparent films with a controllable density. The thin films were deposited using a sub-stoichiometric TiO_{2-x} target sputtered in pure Ar at different pressures. Subsequent heat treatments at different temperatures were performed to crystallize the amorphous films in the anatase phase. The aim of this study was to investigate the effect of the deposition conditions on the structural and photocatalytic properties of the thin films before and after heat treatment.

2. Experimental

Thin films of TiO_2 were deposited by d.c. magnetron sputtering in a custom made vacuum chamber using a cylindrical magnetron (von Ardenne PPS50). A conductive substoichiometric TiO_{2-x} target of ∅ 50 mm was used (provided by ITME Warsaw, Poland). Before deposition the chamber was pumped to a base pressure below 10^{-3} Pa. Sputtering was performed in pure Ar (sputter gas) at a constant power of 180 W (Hüttinger PFG1500). The target-to-substrate distance was 10 cm; the deposition temperature did not exceed 325 K (self-heating due to deposition). The thin films were deposited onto microscope glass slides at four different Ar pressures, namely 0.1, 0.3, 0.6 and 1.0 Pa. A deposition time of 30 min was chosen to achieve a film thickness close to 300 nm; the exact value was measured using a profilometer (Taylor–Hobson Talystep). For all deposition pressures three samples were heat treated after deposition at temperatures of 673, 723 and 773 K in air to achieve crystallization in the anatase structure.

All as-deposited as well as heat treated films were analyzed. XRD analysis was performed with a diffractometer (Siemens Kristalloflex DS5000) using CuKα radiation at 40 kV and 40 mA working in the $\theta-2\theta$ mode. An estimate of the crystallite size was performed using the Scherrer formula [5]. For microstructural analysis a scanning electron microscope (FEI Quanta 200F FEG-SEM) was used in the low vacuum mode. Optical analysis was performed with a UV–VIS–NIR spectrophotometer (Varian Cary 500) in the wavelength range of 250–2000 nm in transmission mode. The refractive index was calculated using the envelopes of the interference fringes in the transmission spectra, following the method of Swanepoel [6]. ESCA analysis (Perkin Elmer PHI ESCA 5500) was performed to determine the stoichiometry of the as-deposited films.

Measurement of the photocatalytic activity was performed in a custom made stainless steel batch reactor with a volume of 8.75 l. The reaction chamber was first evacuated and then backfilled with an inert Ar/O_2 atmosphere (ratio 80:20 to simulate air) at 1.05×10^5 Pa. The thin films were illuminated at a distance of 15 cm with light from a mercury high-pressure short arc bulb (Osram HBO 200W/2) set to 100 W, which passed first through an IR filter (60 mm water). The light entered the reaction chamber through a glass window (transparent for $\lambda>300$ nm). Therefore the active peak wavelength of the UV lamp is $\lambda=365$ nm. The thin films were characterized by measuring the photocatalytic breakdown of 273 ppm ethanol using an atmospheric gas analyzer containing a mass spectrometer (Pfeiffer Vacuum Omnistar). The temperature during the reaction process was 313 K. The illuminated thin film area was 31×25 mm^2.

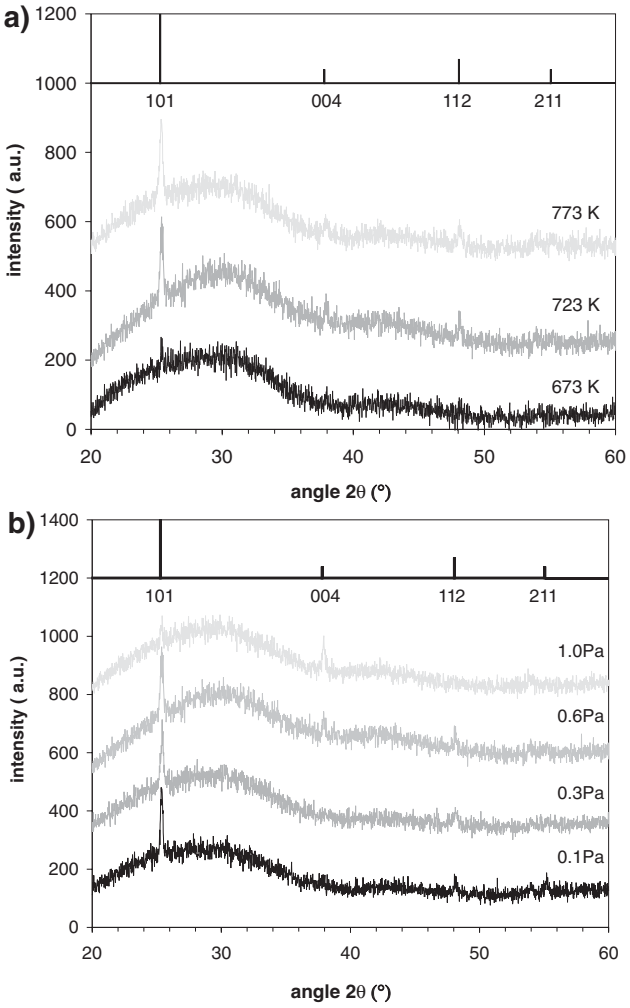

Fig. 2. Dependence of crystal structure on (a) anneal temperature (deposition pressure 0.6 Pa), (b) deposition pressure (annealed at 723 K). The sharp lines show the major peak positions and intensities for powder anatase (ASTM 21-1272).

3. Results and discussion

3.1. Structural properties

ESCA analysis based on the Ti2p photo-electron shape revealed only Ti^{4+}. From this result it can be concluded that the as-deposited films are as good as stoichiometric, even though they were sputtered without additional oxygen.

3.1.1. Dependence of deposition thickness and refractive index on Ar-gas pressure

The deposition rate as a function of the deposition pressure goes through a maximum (Fig. 1). This follows the general trend observed in magnetron sputtering that at low pressures less ionization and, therefore, a lower sputter rate is observed. At high pressures the gas density increases which increases scattering of the sputtered particles resulting in less particles arriving at the substrate [7].

In Fig. 1 can be seen that for the as-deposited films as well as for the annealed films the refractive index (at $\lambda = 550$ nm) decreases with increasing sputter pressure. For the as-deposited films the values of n show the largest spreading, going from almost 2.5 at 0.1 Pa to 1.9 at 1.0 Pa. This indicates that there is a decrease in film density with increasing deposition pressure. With increasing anneal temperature the refractive index decreases for films deposited at 0.1 Pa, while for films at 1 Pa it increases, resulting in a more similar refractive index, and a more similar density, for the different films. The literature values for sputtered crystalline anatase thin film and single crystal anatase are 2.4 [8] and 2.5 [9], respectively. The as-deposited film sputtered at 0.1 Pa, which is XRD amorphous (see next section), has a refractive index higher than the one reported for a crystalline anatase thin film, reaching the single crystal value.

3.1.2. XRD analysis

Fig. 2a summarizes the dependence of the film structure on the anneal temperature for the deposition pressure of 0.6 Pa. As-deposited films (not shown) and films annealed at 673 K are XRD amorphous. Films heat treated at temperatures of 723 K and higher are crystalline, showing only peaks from the anatase crystal structure. For a given deposition pressure no significant difference between the highest two anneal temperatures was observed.

Fig. 2b shows the $\theta-2\theta$ XRD spectra for the films annealed at 723 K. Films deposited at 0.1, 0.3 and 0.6 Pa show a stronger (101) peak than expected from the powder spectrum, indicating a preferential crystallization in the (101) direction. The films deposited at 1.0 Pa crystallize completely differently. Here the normally dominant (101) peak has become less intense than the (004) peak, indicating a strong (001) orientation. This means that the crystallographic orientation of the films is controlled by the deposition conditions and not by the anneal temperature.

For the films sputtered at 0.1, 0.3 and 0.6 Pa an estimate of the crystallite size for the (101) reflection at 25.3° could be performed using the Scherrer formula. The film deposited at 0.1 Pa and annealed at 773 K has a larger crystallite size (122 nm) than the other films (between 40 and 70 nm).

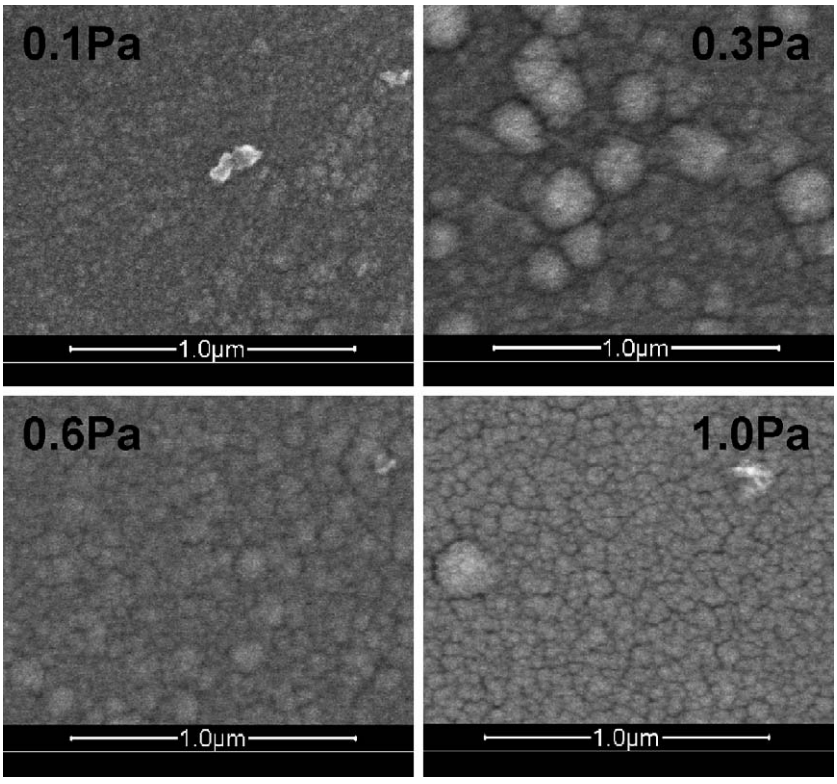

Fig. 3. SEM images of as-deposited films for deposition pressures of 0.1, 0.3, 0.6 and 1.0 Pa.

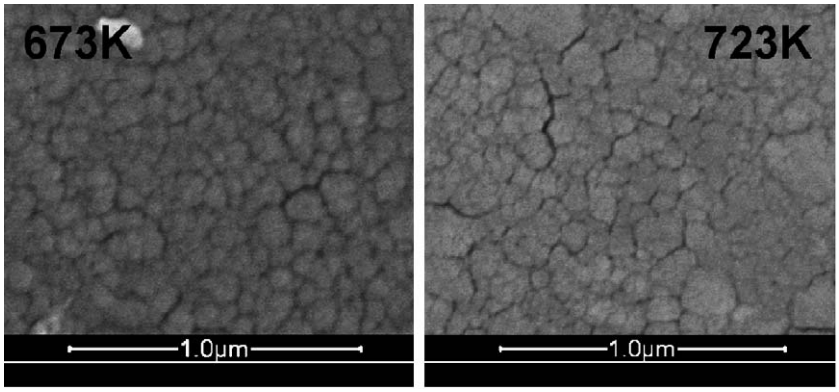

Fig. 4. SEM images of films annealed at 673 and 723 K (deposited at 0.6 Pa).

3.1.3. SEM analysis

Fig. 3 shows the microstructure (top view) of the as-deposited films for different pressures. It can be seen that the films become less dense with increasing deposition pressure, the films deposited at 0.6 and 1.0 Pa showing grooves between the grains. There is very little difference observed between the annealed films. As an example films annealed at 673 and 723 K (0.6 Pa) are shown in Fig. 4. These films show stronger grooving along the grain boundaries compared to the as-deposited film (Fig. 3). The average grain size of all films is estimated to be about 50 nm. When comparing to the crystallite size estimated from XRD measurements, one can see that the crystallite size is of the order of the grain size. An exception is the film deposited at 0.1 Pa, annealed at 773 K which has a crystallite size larger than 100 nm. Here one must remember that grains may extend deep into the film. Unfortunately, SEM cross-sectional views of the films (fractured surfaces) showed no details on the film structure.

3.2. Photocatalytic properties

In Fig. 5a the photocatalytic breakdown of ethanol is shown for the as-deposited films. The film deposited at 0.1 Pa shows very little activity, but up to 0.6 Pa the decomposition rate increases with increasing deposition pressure. The increase in photocatalytic activity with deposition pressure follows the more open structure, which is seen in the SEM images (Fig. 3) and the reduced density indicated by the refractive indices (Fig. 1). However, the film deposited at 1.0 Pa does not show any improvement in photocatalytic activity. There is no clear correlation between the estimated grain or crystallite sizes and the photocatalytic activity for these films.

For the most active films it takes 9 h to reduce the ethanol concentration by one third. In the same system a spin coated layer of P25 (effective surface area ca. 50 m^2/g [4,10]) having the same sample area completely mineralizes the same amount of ethanol in about 2 h. Due to its powder nature the P25 has a very open structure (films appear white), so that it is difficult to compare with the smooth, transparent sputtered films.

Post deposition heat treatment changes the photocatalytic activity of the films without influencing the pressure dependence. This is shown for the films deposited at 0.6 Pa in Fig. 5b. The film heat treated at a temperature of 723 K shows the highest activity, decreasing the concentration of ethanol by almost one half after 9 h of illumination. The films deposited at 673 and 773 K both show a lower activity than the as-deposited film. We suspect that there are two competing effects: The first is improvement of the photocatalytic activity due to crystallization. The second is diffusion of Na-ions from the glass substrate into the film, which deteriorates the photocatalytic activity of anatase TiO_2 [11]. To avoid Na-contamination one can use sodium-free glass or a buffer coating of SiO_2 on soda–

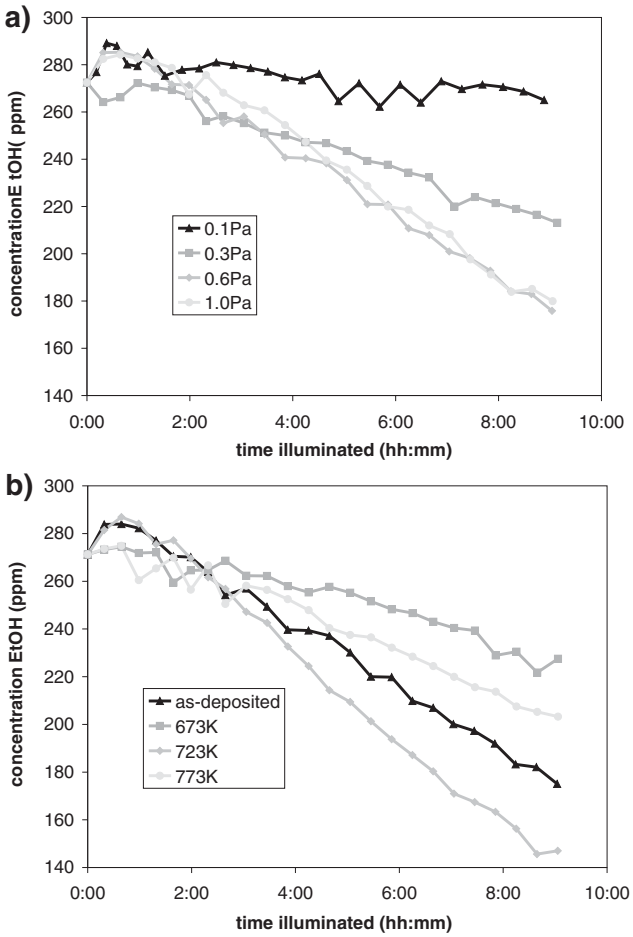

Fig. 5. Photocatalytic activity of sputtered thin films: (a) as-deposited, sputtered at different pressures, (b) deposited at 0.6 Pa, effect of heat treatment.

lime glass [12]. More detailed studies of the photocatalytic activity using inert glass are planned for the future.

4. Conclusions

Stoichiometric TiO_2 thin films have been deposited by d.c. magnetron sputtering from a sub-stoichiometric TiO_{2-x} target at different Ar pressures. The influence of the pressure on the refractive index, the microstructure and the photocatalytic activity was investigated. The values for the refractive index and the SEM images of the microstructure indicate that the film density decreases with increasing sputtering pressure. Crystallization in the anatase structure is seen for films annealed at temperatures of 723 K and higher, and the preferred orientation is seen to change from (101) at lower pressures (0.1–0.6 Pa) to (001) at higher pressures (1.0 Pa). The most photocatalytic active film is the one deposited at 0.6 Pa, heat treated at 723 K. From this it can be concluded that a more open structure is beneficial for the photocatalytic activity of anatase TiO_2. The effect of grain orientation and film thickness will be subjects of further studies.

Acknowledgements

The authors are grateful to Ulric Demeter for performing the XPS measurements and Olivier Janssens for performing the SEM measurements. This research was performed in the framework of a Concerted Research Action (GOA) financed by the Ghent University.

References

[1] O. Carp, C.L. Huisman, A. Reller, Prog. Solid State Chem. 32 (2004) 33.
[2] A. Mills, S. Le Hunt, J. Photochem. Photobiol., A Chem. 108 (1997) 1.
[3] T. Ohno, K. Tokieda, S. Higashida, M. Matsumara, Appl. Catal., A Gen. 244 (2003) 383.
[4] M. Anpo, M. Takeuchi, J. Catal. 216 (2003) 505.
[5] B.D. Cullity, Elements of X-ray Diffraction, 2nd edition, Addison-Wesley Publishing Company, 1978.
[6] R. Swanepoel, J. Phys. E: Sci. Instrum. 29 (1983) 1214.
[7] J.A. Thornton, A.S. Penfold, in: J.L. Vossen, W. Kern (Eds.), Thin Film Processes, Academic Press, 1978, Chapter II-2.
[8] S. Schiller, G. Beister, S. Schneider, W. Sieber, Thin Solid Films 72 (1980) 475.
[9] CRC Handbook of Chemistry and Physics, 82nd edition, CRC Press, Boca Raton (2001–2002).
[10] Degussa Aerosil, Product information Aeroxide TiO_2 P25.
[11] A. Fernández, G. Lassaletta, V.M. Jiménez, A. Justo, A.R. González-Elipe, J.-M. Herrmann, H. Tahiri, Y. Ait-Ichou, Appl. Catal., B Environ. 7 (1995) 49.
[12] S. Takeda, S. Suzuki, H. Odaka, H. Hosono, Thin Solid Films 392 (2001) 338.